npg

p66SHC promotes T cell apoptosis by inducing mitochondrial dysfunction and impaired Ca^{2+} homeostasis

M Pellegrini[1,4], F Finetti[1,4], V Petronilli[2], C Ulivieri[1], F Giusti[1], P Lupetti[1], M Giorgio[3], PG Pelicci[3], P Bernardi[2] and CT Baldari*[,1]

p66Shc, a redox enzyme that enhances reactive oxygen species (ROS) production by mitochondria, promotes T cell apoptosis. We have addressed the mechanisms regulating p66Shc-dependent apoptosis in T cells exposed to supraphysiological increases in [Ca^{2+}]$_c$. p66Shc expression resulted in profound mitochondrial dysfunction in response to the Ca^{2+} ionophore A23187, as revealed by dissipation of mitochondrial transmembrane potential, cytochrome c release and decreased ATP levels. p66Shc expression also caused a dramatic alteration in the cells' Ca^{2+}-handling ability, which resulted in Ca^{2+} overload after A23187 treatment. The impairment in Ca^{2+} homeostasis was ROS dependent and caused by defective Ca^{2+} extrusion due at least in part to decreased plasma membrane ATPase (PMCA) expression. Both effects of p66Shc required Ca^{2+}-dependent serine-36 phosphorylation. The mitochondrial effects of p66Shc were potentiated by but not strictly dependent on the rise in [Ca^{2+}]$_c$. Thus, Ca^{2+}-dependent p66Shc phosphorylation causes both mitochondrial dysfunction and impaired Ca^{2+} homeostasis, which synergize in promoting T cell apoptosis.

p66Shc is a splice variant of p52Shc/p46Shc, a cytosolic adaptor controlling mitogenic signaling from tyrosine kinases to Ras.[1] Although the domain organization is identical in the three isoforms, p66Shc not only fails to activate Ras, but competitively inhibits signaling by the other isoforms.[2–4] Furthermore, p66Shc is implicated in signaling pathways linking oxidative stress to apoptosis.[5] This property maps to a unique N-terminal domain containing a critical serine residue at position 36, which is phosphorylated in response to stress.[4,6–8] Inactivation of the gene encoding p66Shc in the mouse results in prolonged life span,[6] which has been ascribed to a decreased production of reactive oxygen species (ROS).[9,10] Furthermore, p66Shc gene ablation results in protection from oxidative stress-related pathologies in mouse disease models, including high-fat-diet-induced atherogenesis[11] and muscular and endothelial cell apoptosis in acute ischemia.[12]

p66Shc-mediated apoptosis is strictly related to oxidative stress and induction of the intrinsic, mitochondrial pathway.[6,10] A fraction of p66Shc localizes to mitochondria as a complex with Hsp70, wherefrom it is released upon UV irradiation.[13] Mitochondrial p66Shc increases ROS production and favors opening of the permeability transition pore (PTP),[13] a high-conductance inner membrane channel involved in the apoptotic response to a number of stimuli.[14] The mechanism whereby p66Shc mediates mitochondrial ROS production has been recently clarified with the demon-stration that p66Shc is a redox enzyme able to oxidize cytochrome c and produce H$_2$O$_2$, causing PTP opening and apoptosis.[15]

Unlike p52Shc/p46Shc, which are ubiquitously expressed, p66Shc is not expressed in neurons and hemopoietic cells as a result of promoter methylation.[16] We have, however, shown that T cells express p66Shc in response to a variety of apoptogenic stimuli, resulting in sensitization to apoptosis. Conversely, inactivation of the *p66Shc* gene protects T cells from dexamethasone-induced apoptosis.[4] Here, we have investigated the mechanisms whereby p66Shc primes T cells to death by the Ca^{2+} ionophore A23187, a potent inducer of apoptosis that causes PTP opening in other systems.[17] We show that p66Shc promotes T cell apoptosis both by triggering cytochrome c release and mitochondrial membrane depolar-ization, and by impairing Ca^{2+} homeostasis due to down-regulation of plasma membrane ATPases and defective Ca^{2+} extrusion. These two independent activities, which both require Ca^{2+}-dependent p66Shc phosphorylation at S36, are likely to synergize in mediating p66Shc-dependent apoptosis.

Results

p66Shc sensitizes T cells to apoptosis by impairing mitochondrial integrity. The apoptogenic activity of p66Shc in fibroblasts has been ascribed to its capacity to

promote production of ROS which, by inducing PTP opening, cause mitochondrial damage, cytochrome *c* release and activation of the caspase cascade.[10,13,15] To understand the mechanisms underlying T cell priming to apoptosis by p66Shc, we used Jurkat T cell transfectants stably expressing either wild-type p66Shc or a substitution mutant where S36 was mutated to alanine (p66SA) (Figure 1a). Apoptosis was induced using the Ca^{2+} ionophore A23187. In agreement with previous results,[4] p66Shc potentiated A23187-induced cell death, as measured both by annexin-V staining (Figure 1b) and by Trypan Blue exclusion (Figure 1c). Interestingly, untreated p66Shc-expressing cells displayed unique morphological features compared to control cells, including accumulation of lipid vesicles, abundant cytoplasmic protrusions at the cell surface and – of particular relevance to the apoptogenic activity of p66Shc – significant amounts of dense heterochromatin (Figure 1d).
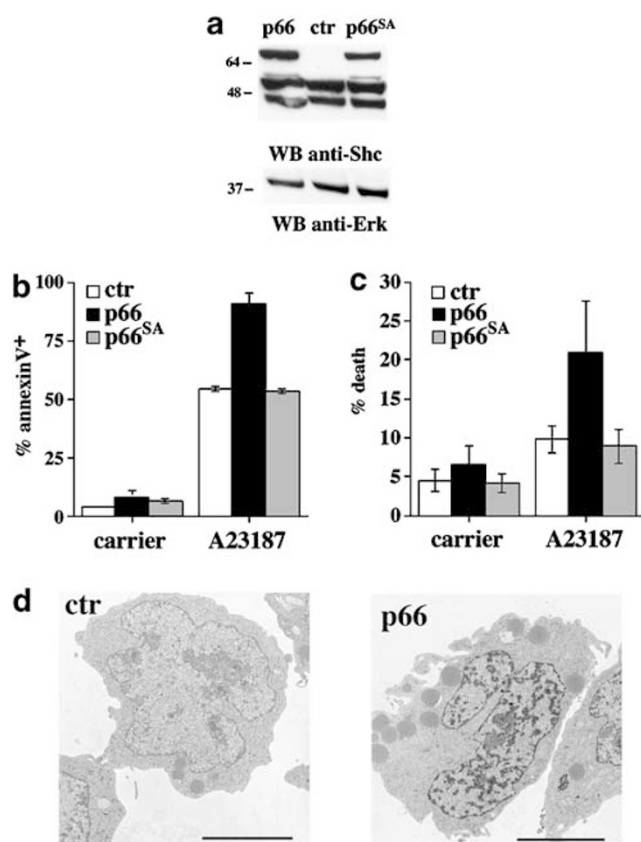

Figure 1 p66Shc expression enhances Jurkat T-cell susceptibility to A23187-induced apoptosis. (**a**) Immunoblot analysis using anti-Shc antibodies of postnuclear supernatants of Jurkat cells stably transfected with empty vector (ctr) or with expression constructs encoding either wild-type p66Shc (p66) or a mutant carrying a serine to alanine substitution at position 36 (p66SA). The migration of molecular mass markers is indicated. (**b**) Quantitation by flow cytometry of annexin V staining on control or p66Shc/p66SA-expressing cells after treatment for 20 min with either carrier or 500 ng/ml A23187. The graph shows the % of annexin-V$^+$ cells (*n* = 3). (**c**) Quantitation of cell death by Trypan blue exclusion in the same T-cell lines after treatement for 6 h in serum-free medium with either carrier or 500 ng/ml A23187 (*n* > 3). (**d**) Electron micrographs of thin sections of untreated control and p66Shc-expressing cells. The size bar indicates 5 μm. Representative cells are shown

To assess whether p66Shc triggers the mitochondrial apoptosis pathway in T cells, mitochondrial integrity was monitored using the fluorescent probe tetramethylrhodamine methyl ester (TMRM), which accumulates in energized mitochondria wherefrom it is released upon membrane depolarization. Flow cytometric analysis of TMRM fluorescence revealed that A23187 treatment caused rapid and complete mitochondrial depolarization in p66Shc-expressing, but not in control cells (Figure 2a). In agreement with a mitochondrial involvement in the amplification by p66Shc of A23187-induced apoptosis, release of cytochrome *c* was strongly enhanced in p66Shc-expressing cells (Figure 2b). Furthermore, measurement of cellular ATP showed not only the expected reduction in both cell lines following A23187 treatment but also significantly lower ATP levels in untreated p66Shc-expressing cells compared to controls (Figure 2c). Of note, enhancement of mitochondrial depolarization and cytochrome *c* release by p66Shc, which correlated with enhanced apoptosis, was also found in cells triggered to undergo activation-induced death (AICD) by prolonged TCR/ CD3 ligation (Figure 3). Hence, p66Shc expression results in mitochondrial dysfunction.

Electron microscopic analysis revealed that the mitochondrial morphology of untreated control and p66Shc-expressing cells was similar, with an electron-transparent matrix and thin, tubular *cristae*. A23187 treatment resulted in increased electron density of the mitochondrial matrix in both cell types, a change that in p66Shc-expressing cells was accompanied by the presence of fewer *cristae* of larger dimensions and by a marked increase of the intercristal space, indicative of extensive mitochondrial remodeling. A23187 treatment also led to defects of the inner and outer mitochondrial membranes, resulting in the absence of a clear boundary between matrix and cytosol, which was particularly striking in p66Shc-expressing cells (Figure 2d).

p66Shc induces apoptosis in fibroblasts by triggering PTP opening.[13] Opening of the PTP in response to a number of stimuli, including Ca^{2+}, arachidonic acid and ROS, results in osmotic swelling of the mitochondria followed by outer membrane rupture, cytochrome *c* release, ATP depletion and cell death.[18] To investigate the potential role of PTP opening in mitochondrial membrane permeabilization and cytochrome *c* release in T cells, p66Shc-expressing cells were treated with cyclosporin A (CsA), which desensitizes the PTP by interacting with cyclophilin D.[18] Neither the kinetics nor the extent of mitochondrial depolarization were modified by CsA (Figure 2e). Similar results were obtained after treatment with sanglifehrin A, another PTP inhibitor that targets cyclophilin D (results not shown), suggesting that PTP opening may not play a major role in mitochondrial depolarization associated with p66Shc expression in A23187-treated cells. This possibility was further explored using a different approach to modulate PTP function. We have previously shown that in hepatoma cells A23187 triggers Ca^{2+}-dependent PTP opening through activation of cytosolic phospholipase A2 (cPLA$_2$) and production of arachidonic acid.[17] We therefore tested whether A23187-induced mitochondrial depolarization in p66Shc-expressing cells could be inhibited by the cPLA$_2$ inhibitor aristolochic acid or potentiated by inhibition of 5-lipoxygenase by MK886 and cyclooxygenases
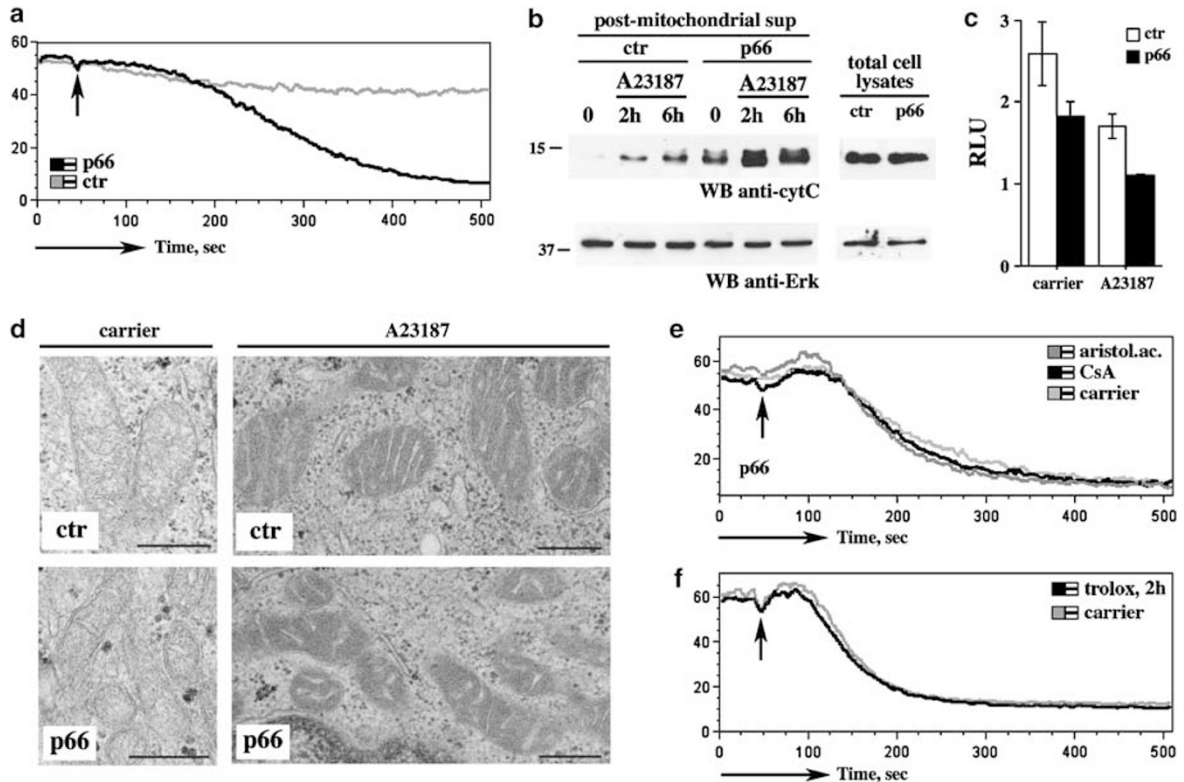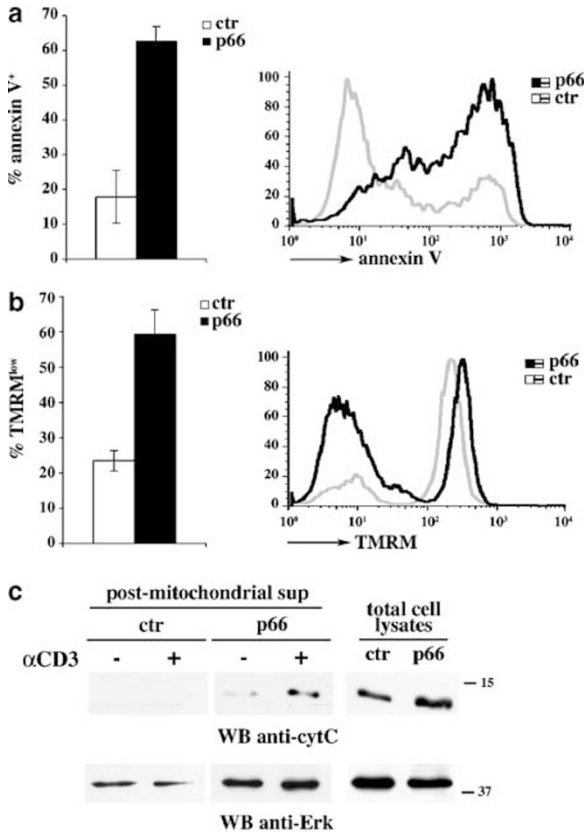
Figure 2 p66Shc expression results in mitochondrial dysfunction. (**a**) Flow cytometric analysis of mitochondrial membrane potential in TMRM-loaded control (gray line) and p66Shc-expressing (black line) Jurkat cells. TMRM was loaded to a comparable extent in both cell lines, as evaluated by fluorimetric analysis of cells lysed with digitonin (not shown). The arrow indicates the time of addition of A23187 (top) or anti-CD3 mAb (bottom). Representative experiments are shown ($n>3$). (**b**) Immunoblot analysis using cytochrome c antibodies of post-mitochondrial supernatants of lysates from control and p66Shc-expressing Jurkat cells either untreated or stimulated for the indicated times with 500 ng/ml A23187. As control of anti-cytochrome c expression in the two cell transfectants, a blot on total cell lysates is shown on the right. Control blots of the stripped filters are shown below. The migration of molecular mass markers is indicated ($n>3$). (**c**) Relative levels of ATP in control and p66Shc-expressing cells treated with either carrier or 500 ng/ml A23187 for 20 min. RLU, relative light units ($n=3$). (**d**) Electron micrographs of thin sections of control and p66Shc-expressing cells, treated for 20 min with either carrier or 500 ng/ml A23187. The size bar represents 0.3 μm. Representative images are shown. (**e, f**) Flow cytometric analysis of mitochondrial membrane potential in TMRM-loaded p66Shc-expressing cells treated with 500 ng/ml A23187 after a 30 min pretreatment with carrier (light gray line), 50 μM aristolochic acid (dark gray line) or 1 μg/ml CsA (black line) (**e**), or a 2 h pretreatment with carrier (light gray line) or 2 mM Trolox (black line) (**f**). The arrow indicates the time of addition of A23187 ($n \geqslant 3$)

by indomethacin, a treatment that results in arachidonic acid accumulation.[17] These treatments did not affect the mitochondrial membrane potential response to A23187 (Figure 2e and data not shown).

Of note, neither treatment of p66Shc-expressing cells with the antioxidant Trolox, a lipophilic vitamin E analog, or treatment of control cells with H_2O_2, modified to any significant extent the respective kinetics of mitochondrial membrane depolarization in response to A23187 (Figure 2f and data not shown). Hence, while p66Shc triggers the mitochondrial pathway of apoptosis in T cells, the mechanism responsible for mitochondrial recruitment does not appear to involve ROS-dependent PTP opening, at variance with fibroblasts.[13] Trolox treatment abrogated however the enhanced apoptotic response to A23187 of p66Shc-expressing cells (Figure 4), suggesting a role for p66Shc-dependent ROS production in additional apoptotic pathways independent of mitochondria. Support to this hypothesis comes from the functional analysis of the p66Shc S36 mutant (p66SA). Phosphorylation of this residue has been shown to be essential for the apoptogenic activity of p66Shc ([4,6,7] and Figure 1), but not for the oxidizing activity of the mitochondrial pool of the protein.[15] As opposed

to its wild-type counterpart, p66SA expression did not induce mitochondrial dysfunction in A23187-treated cells, as assessed by lack of mitochondrial depolarization (Figure 5a) and cytochrome c release (Figure 5b). As S36-phosphorylated p66Shc is only found in the cytosol,[15] the data collectively indicate that p66Shc triggers not only the mitochondrial pathway of apoptosis but also an additional, extramitochondrial pathway.

p66Shc impairs Ca^{2+} homeostasis in T cells. By promoting activation of many proapoptotic molecules and expression of proapoptotic genes, Ca^{2+} acts a key player both in the intrinsic and extrinsic apoptosis pathways.[19] Among the latter of particular relevance to T cells is the Ca^{2+}-dependent pathway controlling AICD.[20] To assess whether the proapoptotic activity of p66Shc may be related to alterations in [Ca^{2+}]$_c$, the kinetics of [Ca^{2+}]$_c$ mobilization in response to A23187 was determined by flow cytometric analysis of Fluo-4-loaded cells. Control cells responded with an initial increase in [Ca^{2+}]$_c$, which consistently dropped to lower levels within 2 min. Remarkably, p66Shc-expressing cells underwent a larger early [Ca^{2+}]$_c$ rise that was followed

Figure 3 p66Shc expression enhances mitochondrial dysfunction in AICD. (**a**) Quantitation by flow cytometry of annexin-V staining on control or p66Shc-expressing cells after treatment for 48 h with saturating amounts of plate-bound anti-CD3 mAb ($n = 3$). Representative histograms are shown on the right (control cells, gray line; p66Shc-expressing cells, black line). (**b**) Flow cytometric analysis of mitochondrial membrane potential in TMRM-loaded control or p66Shc-expressing cells treated as above and restimulated for 6 h with anti-CD3 mAb. The graph shows the percentage of depolarized cells (TMRM^{low}) ($n = 3$). Representative histograms are shown on the right (control cells, gray line; p66Shc-expressing cells, black line). (**c**) Immunoblot analysis using cytochrome c antibodies of post-mitochondrial supernatants of lysates from control and p66Shc-expressing Jurkat cells treated as above. As control of cytochrome c expression, a blot on total cell lysates is also shown. Control blots of the stripped filters are shown below

Figure 4 p66Shc-dependent apoptosis requires Ca^{2+} and ROS. Quantitation by flow cytometry of annexin-V staining on control or p66Shc-expressing cells after treatment for 20 min with either carrier or 500 ng/ml A23187. Cells were pretreated for 40 min with EGTA (5 mM) or thapsigargin (2 μM), alone or in combination, or pretreated for 2 h with 2 mM Trolox, or treated for 120 h with 1 μg/ml CsA. The graph shows the % of annexin-V$^+$ cells ($n \geqslant 3$)

by Ca^{2+} deregulation, as shown by a dramatic and sustained further increase in [Ca^{2+}]$_c$ (Figure 6a). Pretreatment with thapsigargin, a drug that depletes intracellular Ca^{2+} stores, normalized the early [Ca^{2+}]$_c$ rise and partially reduced the late phase of [Ca^{2+}]$_c$ increase. On the other hand, pretreatment with EGTA, a cell-impermeant Ca^{2+} chelator, normalized both the early and late [Ca^{2+}]$_c$ responses to A23187 (Figure 6b). These findings indicate that both external Ca^{2+} and intracellular stores contribute to the overwhelming [Ca^{2+}]$_c$ responses of p66Shc-expressing cells. Ca^{2+} depletion by combined treatment with EGTA and thapsigargin, which restored normal Ca^{2+} responses (Figure 6b), fully protected p66Shc-expressing cells from apoptosis (Figure 4), underlining the causal role of the observed Ca^{2+} overload in the enhanced A23187-induced apoptosis of these cells.

Of note, even after treatment with EGTA, alone or in combination with thapsigargin, p66Shc-expressing cells

displayed a larger early [Ca^{2+}]$_c$ increase in response to A23187 (Figure 6c), suggesting that p66Shc increases the Ca^{2+} contents of intracellular stores. In agreement with this possibility, thapsigargin treatment in the absence of A23187 resulted in increased [Ca^{2+}]$_c$ in p66Shc-expressing cells compared to controls (Figure 6d). Furthermore, p66Shc caused a larger increase of [Ca^{2+}]$_c$ after TCR/CD3 engagement. It should be underlined that the TCR/CD3-dependent increase in [Ca^{2+}]$_c$ returned to basal levels with the same time course as that of control cells (Figure 6d), suggesting that p66Shc-expressing cells can handle the relatively modest increase of [Ca^{2+}]$_c$ induced by physiological stimulation but not the massive Ca^{2+} overload induced by A23187.

To understand whether the increased ROS production in p66Shc-expressing cells is implicated in the observed A23187-induced Ca^{2+} deregulation, we measured the kinetics of [Ca^{2+}]$_c$ mobilization in response to A23187 after cell treatment with the antioxidant Trolox. This treatment resulted in a significant amelioration of the Ca^{2+}-handling ability of p66Shc-expressing cells (Figure 6e). Conversely, exposure of control cells to H$_2$O$_2$ resulted in Ca^{2+} deregulation (Figure 6f). Taken together with inability of Trolox to restore mitochondrial integrity in p66Shc-expressing cells (Figure 2f), notwithstanding its protective effect on A23187-induced apoptosis (Figure 4), these data suggest that the ROS-dependent pathway of apoptosis triggered by p66Shc involves Ca^{2+} deregulation. In agreement with the requirement for S36 phosphorylation in p66Shc-dependent apoptosis (Figure 1) and the role of impaired Ca^{2+} homeostasis in this process (Figure 4), cells expressing the p66SA mutant displayed a normal [Ca^{2+}]$_c$ response (Figure 5c).

p66Shc downregulates plasma membrane Ca^{2+} ATPases. Plasma membrane Ca^{2+} ATPases (PMCA) play a key role in Ca^{2+} homeostasis. In lymphocytes, PMCAs represent the principal means to extrude Ca^{2+} that has
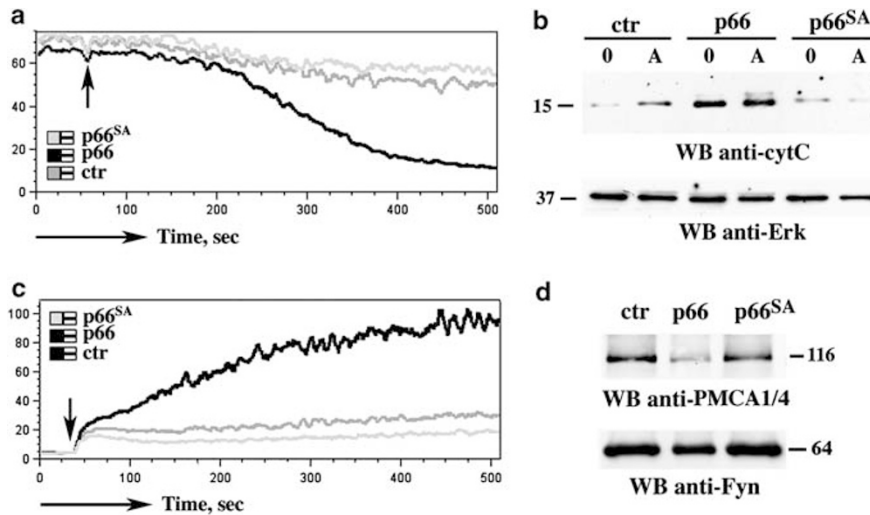
Figure 5 The effects of p66Shc on mitochondrial function and [Ca^{2+}]$_c$ deregulation require serine 36 phosphorylation. (**a**) Flow cytometric analysis of mitochondrial membrane depolarization in TMRM-loaded control or p66Shc/p66SA-expressing Jurkat cells in response to 500 ng/ml A23187. The arrow indicates the time of addition of A23187. Representative experiments are shown ($n > 3$). (**b**) Immunoblot analysis using anti-cytochrome c antibodies of post-mitochondrial supernatants of lysates from control or p66Shc/p66SA-expressing Jurkat cells either untreated or stimulated for 30 min with 500 ng/ml A23187. A control blot of the stripped filter is shown below ($n = 3$). The migration of molecular mass markers is indicated. (**c**) Flow cytometric analysis of [Ca^{2+}]$_c$ in Fluo-4-loaded control (dark gray line) or p66Shc (black line)/p66SA (light gray line)-expressing Jurkat cells in response to 500 ng/ml A23187. The arrow indicates the time of addition of A23187. Representative experiments are shown ($n > 3$). (**d**) Immunoblot analysis of lipid rafts purified from control or p66Shc/p66SA-expressing cells with anti-PMCA1/4 antibodies. After stripping, the filter was reprobed with anti-Fyn antibodies as loading control

entered through CRAC channels[21] and have been shown to underlie attenuation of Ca^{2+} signaling by the inhibitory coreceptor CD22 in B cells.[22] We therefore investigated the expression levels of PMCA1/4, which are the major T cell species. Immunoblot analysis revealed a significant reduction in PMCA1/4 expression in lysates from p66Shc-expressing cells compared to controls (Figure 7a). PMCA1/4 was also analyzed in lipid rafts where these proteins are known to preferentially segregate.[23] Lower PMCA1/4 levels were detected in rafts from p66Shc-expressing cells (Figure 7a). RT-PCR analysis with primers specific for PMCA1b, 4a and 4b revealed a selective reduction in the levels of PMCA4a-specific mRNA (Figure 7b).

Expression of the PMCA4 CII splice variant has been reported to be downregulated at the transcriptional level by the Ca^{2+}/CaM-dependent phosphatase calcineurin.[24] As nuclear translocation of the transcription factor nuclear factor of activated T cells (NF-AT) is exquisitely calcineurin-dependent,[25] we used an NFAT- green fluorescent protein (GFP) fusion protein as a reporter of calcineurin activity. A plasmid encoding NFAT-GFP was transiently transfected into the Jurkat lines, and the number of cells displaying nuclear fluorescence was scored. A larger proportion of p66Shc-expressing cells displayed nuclear localization of NFAT-GFP compared to controls, both under basal conditions and after addition of A23187 (Figure 7c), indicating higher levels of calcineurin activity. To assess whether calcineurin activity was involved in downregulation of PMCA4a gene expression, p66Shc-expressing cells were subjected to long-term (120 h) treatment with CsA, which inhibits calcineurin after binding to cyclophilin A. This treatment led to recovery of PMCA expression to the levels observed in control cells (Figure 7d).

Under these conditions, no Ca^{2+} deregulation was observed after A23187 treatment (Figure 7e), and apoptosis was reduced, although protection was partially offset by toxicity of the immunosuppressant, which can be appreciated by increased apoptosis in control cells (Figure 4).

Cells expressing the p66SA mutant, which did not display any impairment in Ca^{2+} homeostasis, expressed PMCA1/4 to the same levels as control cells (Figure 5d). Furthermore, the relative levels of PMCA4a-specific mRNA in p66SA-expressing cells were comparable to those in controls (96.3% $\pm$ 6.0 of the mRNA levels found in control cells; $n = 3$), as was the proportion of cells harboring basal nuclear NF-AT localization (data not shown). Hence, downregulation of PMCA1/4, resulting at least in part from attenuation of PMCA4a gene transcription, is tightly correlated with the decreased ability of p66Shc-expressing cells to handle the massive Ca^{2+} overload induced by A23187. The important role of PMCAs in the defective p66Shc-dependent Ca^{2+} homeostasis is underlined by the finding that pretreatment of control cells with sodium vanadate, a PMCA inhibitor, resulted in an A23187-induced Ca^{2+} mobilization profile similar to the one observed in p66Shc-expressing cells (Figure 7f).

The effects of p66Shc on mitochondrial integrity and Ca^{2+} homeostasis are independent but both require Ca^{2+}, which is essential for S36 phosphorylation. In addition to promoting PTP opening, Ca^{2+} has other mitochondrial targets implicated in apoptosis, including proapoptotic members of the Bcl-2 protein family such as Bad, which is sequestered in the cytosol through its association with 14-3-3, and cardiolipin, an anionic phospholipid that mediates cytochrome c association with
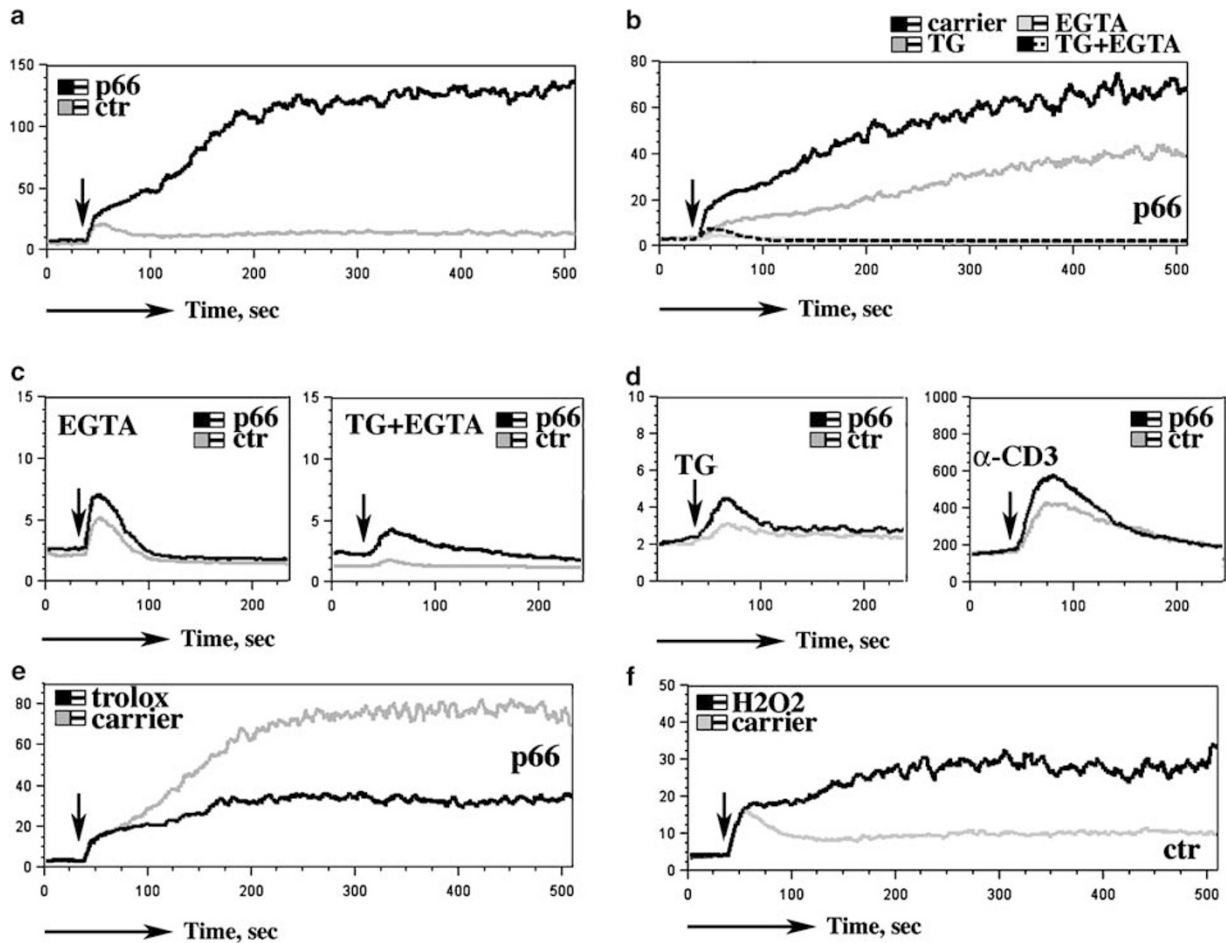
Figure 6 Expression of p66Shc results in [Ca^{2+}]$_c$ deregulation. (**a**) Flow cytometric analysis of [Ca^{2+}]$_c$ in Fluo-4-loaded control (gray line) or p66Shc-expressing (black line) Jurkat cells in response to 500 ng/ml A23187. Fluo-4 was loaded to a comparable extent in both cell lines, as evaluated by fluorimetric analysis of cells lysed with digitonin (not shown). Representative experiments are shown ($n > 3$). (**b**) Flow cytometric analysis of [Ca^{2+}]$_c$ in Fluo-4-loaded p66Shc-expressing Jurkat cells treated with 500 ng/ml A23187 in the presence of carrier (black line), thapsigargin (2 μM) (TG, dark gray line) or EGTA (5mM), alone (light gray solid line) or in combination with thapsigargin (black dashed line). The initial phase of the kinetics of a representative experiment is shown on an expanded scale in panel (**c**). The arrow indicates the time of addition of A23187. (**d**) Flow cytometric analysis of [Ca^{2+}]$_c$ in Fluo-4-loaded control (gray line) or p66Shc-expressing (black line) Jurkat cells treated with either thapsigargin (2 μM) (TG) or anti-CD3 mAb. The arrow indicates the time of addition of the stimulus. (**e**, **f**) Flow cytometric analysis of [Ca^{2+}]$_c$ in Fluo-4-loaded p66Shc-expressing cells treated for 1 h with 2 mM Trolox (**e**) or control cells treated for 40 min with 440 μM H$_2$O$_2$ (**f**). Gray lines, carrier; black lines, Trolox (**e**) or H$_2$O$_2$ (**f**). The arrow indicates the time of addition of A23187. Representative experiments are shown ($n \geqslant 3$)

the inner mitochondrial membrane.[19] To understand whether the Ca^{2+} overload in p66Shc-expressing cells treated with A23187 was responsible for mitochondrial dysfunction, we asked whether long-term treatment of p66Shc-expressing cells with CsA, which results in normalization of the Ca^{2+} response (Figure 7e), would prevent mitochondrial depolarization. Surprisingly, CsA treatment did not modify either the dissipation of the mitochondrial membrane potential (Figure 7g) or the enhancement in cytochrome c release triggered by A23187 (Figure 7h). Taken together with the failure of Trolox to restore mitochondrial function despite the normalization of the Ca^{2+} response (Figures 2f and 6e), the results indicate that, while Ca^{2+} overload is likely to amplify the mitochondrial dysfunction in p66Shc-expressing cells, these two activities are independent.

Surprisingly, depletion of Ca^{2+} by cell treatment with EGTA and thapsigargin, which restored normal Ca^{2+} responses

(Figure 6b), also completely abrogated the mitochondrial depolarization triggered by A23187 (Figure 8a). These findings suggest that, while Ca^{2+} overload and mitochondrial dysfunction are independent effects of p66Shc, Ca^{2+} is required for both. We had previously observed that in Jurkat T cells p66Shc displays a basal level of S36 phosphorylation that can be enhanced by a variety of receptor-mediated and pharmacological stimuli including A23187, all of which cause a transient rise of [Ca^{2+}]$_c$.[4] We hypothesized that the [Ca^{2+}]$_c$ rise could be essential for p66Shc phosphorylation at S36. We therefore measured the effect of A23187, H$_2$O$_2$ and CD3 ligation on p66Shc phosphorylation at S36 in Ca^{2+}-competent cells and after Ca^{2+} depletion by treatment with thapsigargin and EGTA. p66Shc phosphorylation was abolished by this treatment in all conditions tested (Figure 8b). While suppression of phosphorylation by A23187 was predictable, it is striking that Ca^{2+} depletion suppressed the

basal level of phosphorylation and prevented its enhancement by stimuli that do not affect Ca^{2+} mobilization directly. These results demonstrate that Ca^{2+} is strictly required for p66Shc phosphorylation by physiological and pharmacological stimuli. This requirement is likely to underlie the Ca^{2+} dependency of both mitochondrial dysfunction and impaired Ca^{2+} homeostasis associated with p66Shc expression.

Discussion

Our data show that p66Shc sensitizes T cells to Ca^{2+}-dependent apoptosis through two distinct activities. The first involves mitochondrial dysfunction, as revealed by cytochrome *c* release, dissipation of mitochondrial transmembrane potential, impaired ATP production and morphological alterations. Although loss of mitochondrial integrity is evident only following A23187 treatment, release of cytochrome *c*, as well as decreased ATP levels, can be observed even under basal conditions, albeit to a lower extent, suggesting that the apoptotic machinery is primed and can be readily recruited in response to apoptotic insults in the presence of p66Shc. This finding is in agreement with the higher frequency of p66Shc-expressing cells with apoptotic morphology compared to control cells. We have previously reported that, by affecting gene expression, p66Shc causes an imbalance between the proapoptotic/antiapoptotic Bcl-2 family members, with a reduction in Bcl-x$_L$ and an increase in Bax expression.[4] By oligomerizing with Bak, Bax forms pores in the outer mitochondrial membrane, resulting in cytochrome *c* release,[26] which was also observed following enforced Bax or Bak expression.[27] Cytochrome *c* release in turn decreases the rate of electron transfer and increases production of the superoxide anion,[28] events that explain the observed mitochondrial depolarization and decreased ATP synthesis. Thus, increased Bax expression may underlie the mytochondrial dysfunction in p66Shc-expressing cells. Both the increased basal Ca^{2+} levels and the enhanced ROS production in these
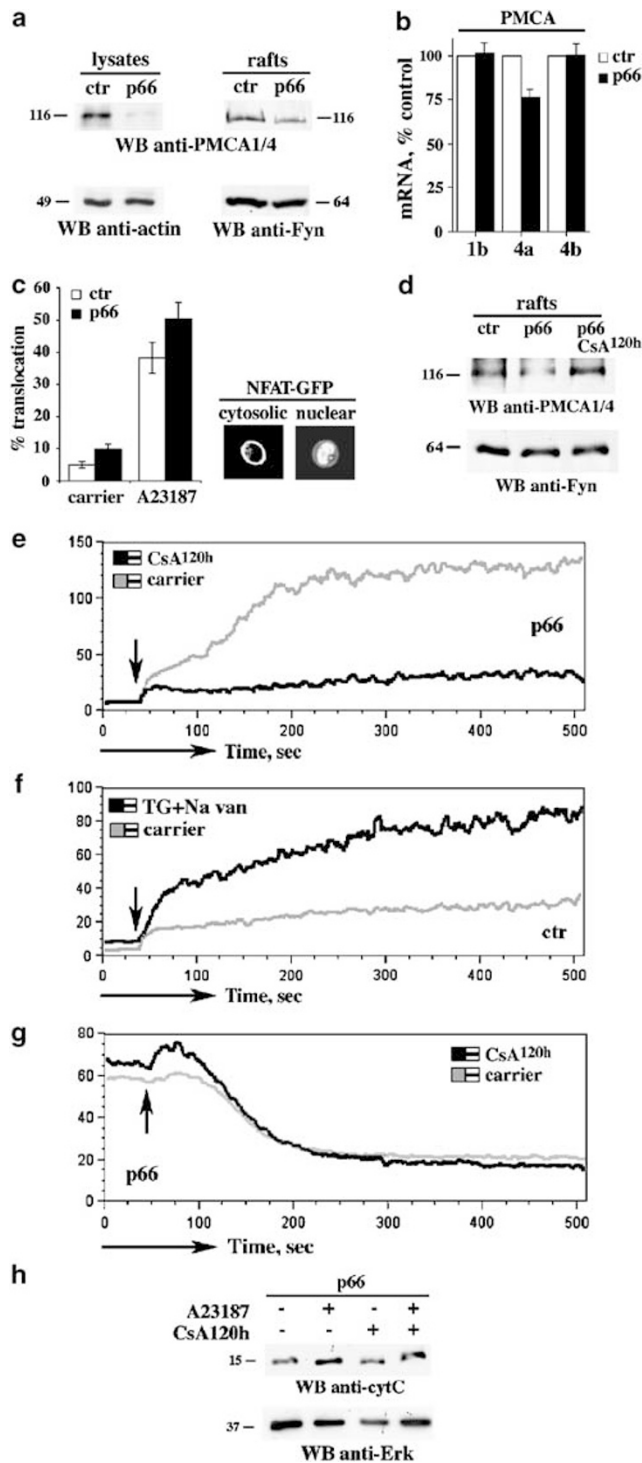
Figure 7 Downregulation of PMCA4a by p66Shc. (**a**) Immunoblot analysis using anti-PMCA1/4 antibodies of postnuclear supernatants (left) or purified lipid rafts (right) of untreated control or p66Shc-expressing Jurkat cells. After stripping, the filters where reprobed with anti-actin (left) or anti-Fyn (a raft resident protein) antibodies as loading control. The levels of reduction of PMCA4a were reproducibly ∼40%, as determined by laser densitometry ($n=3$). (**b**) Semiquantitative RT-PCR analysis of PMCA 1b, 4a and 4b mRNA levels in untreated control and p66Shc-expressing Jurkat cells. RT-PCR products were resolved by agarose gel electrophoresis, quantitated by laser densitometry and normalized to the levels of actin mRNA used as internal control. The data are expressed as % of PMCA-specific mRNA in p66-expressing cells *versus* control cells (taken as 100%) ($n>3$). (**c**) Confocal microscopy of control or p66Shc-expressing Jurkat cells transiently transfected with an NFAT/GFP expression construct, treated for 30 min with either carrier or 500 ng/ml A23187. GFP-positive cells (50–100/sample) showing nuclear NFAT/GFP were scored ($n>3$). The graph shows the % of cells harboring nuclear GFP. Representative images are shown on the right. (**d**) Immunoblot analysis of lipid rafts with anti-PMCA1/4 antibodies (bottom) of p66Shc-expressing cells treated for 120 h with either carrier or 1 µg/ml CsA. The levels of PMCA4a in p66Shc-expressing cells in the representative experiment shown were ∼40% compared to the levels in control cells in the absence of CsA, while they increased to ∼90% after long-term treatment with CsA, as determined by laser densitometry ($n=3$). (**e, f**) Flow cytometric analysis of [Ca^{2+}]$_c$ in Fluo-4-loaded p66Shc-expressing Jurkat cells treated for 120 h with carrier (gray line) or 1 µg/ml CsA (black line) (**e**) or for 40 min with 2 µM thapsigargin (TG) and 1 mM sodium vanadate (Na van) (black line) (**f**). The arrow indicates the time of addition of A23187 ($n>3$). (**g**) Flow cytometric analysis of mitochondrial membrane potential in TMRM-loaded p66Shc-expressing cells treated with 500 ng/ml A23187 after a long-term (120 h) treatment with carrier (gray line) or 1 µg/ml CsA (black line). The arrow indicates the time of addition of A23187 ($n=3$). (**h**) Immunoblot analysis using anti-cytochrome *c* antibodies of post-mitochondrial supernatants of lysates from p66Shc-expressing Jurkat cells either untreated or stimulated for 30 min with 500 ng/ml A23187 after a 120 h incubation with either carrier or 1 µg/ml CsA. A control blot of the stripped filter is shown below ($n=2$). The migration of molecular mass markers is indicated
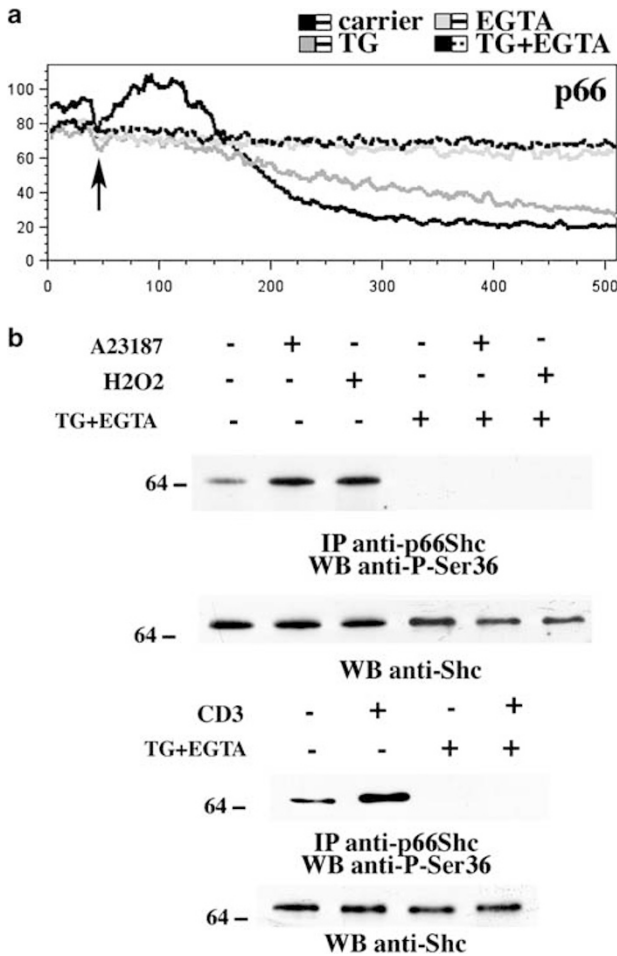
Figure 8 Serine 36 phosphorylation requires Ca^{2+}. (**a**) Flow cytometric analysis of mitochondrial membrane potential in TMRM-loaded p66Shc-expressing cells treated with 500 ng/ml A23187 in the presence carrier (black line), thapsigargin (2 μM) (TG, dark gray line) or EGTA (5 mM) (light gray line), alone or in combination with thapsigargin (black dashed line). The arrow indicates the time of addition of A23187. Representative experiments are shown ($n \geqslant 3$). (**b**) Immunoblot analysis with a serine 36 phosphospecific antibody of p66Shc-specific immunoprecipitates from p66Shc-expressing Jurkat cells treated for 30 min with A23187 (500 ng/ml), H$_2$O$_2$ (440 μM) (top) or 20 min with anti-CD3 mAb (bottom). Control blots of the stripped filters are shown below

cells may further facilitate cytochrome c release by favoring its dissociation from cardiolipin.[19]

The pharmacological evidence presented suggests that PTP opening does not play a major role in p66Shc-dependent mitochondrial membrane depolarization and triggering of the intrinsic apoptotic pathway in A23187-treated T cells. This was somewhat surprising, given that A23187 activates cPLA$_2$ resulting in arachidonic acid production,[17] and that p66Shc increases ROS production,[9,10] events which both contribute to increase the probability of PTP opening. We cannot, however, fully exclude PTP involvement in mitochondrial depolarization, particularly in the light of the ultrastructural changes detectable after treatment with A23187. Mitochondrial *cristae* remodeling has indeed been observed in t-Bid-dependent apoptosis triggered by PTP opening.[29] Furthermore, PTP opening may occur even in the presence of CsA at increasing Ca^{2+} loads.[30]

In addition to its effects on mitochondria, our data show that p66Shc impairs Ca^{2+} homeostasis in T cells. Although in most experiments we have exploited the amplifying effects of A23187, it should be stressed that a clear effect can be detected even under basal conditions. Indeed, higher basal levels of store-associated Ca^{2+} can be detected in p66Shc-expressing cells. Furthermore, these cells display increased nuclear NF-AT translocation, which is likely to cause the observed transcriptional downregulation of PMCA4a. Inhibition of calcineurin has been indeed found to suppress PMCA4 expression in neurons.[24] Our demonstration that calcineurin inhibition by long-term CsA treatment restores PMCA expression strongly suggests that such a mechanism may be operational, although additional effects of CsA, such as reduction of ROS production,[31] cannot be excluded. The moderate reduction in PMCA4a-specific mRNA in p66Shc-expressing cells compared to the reduction in protein suggests that PMCA1/4 expression may be controlled by additional, post-transcriptional mechanisms. PMCAs have been identified in other cell types as targets of both caspases and the Ca^{2+}-dependent protease, calpain.[32,33] Ca^{2+} over-load by A23187 in p66Shc-expressing cells could, however, not be rescued by pharmacological inhibition of either caspases or calpain (unpublished results), ruling out a major role of these proteases in PMCA inactivation. An alternative possibility is suggested by the finding that Ca^{2+} treatment of T cells results in the calcineurin-dependent, CsA-sensitive upregulation of the E3 ubiquitin ligases, Cbl-b, Itch and Grail,[34] that might potentially be implicated in an alternative pathway of PMCA degradation. A second effect of p66Shc expression on Ca^{2+} homeostasis may be mediated by its ability to promote ROS formation,[9,10] leading to functional inactivation of PMCAs.[35] The substantial recovery of the Ca^{2+}-handling ability of p66Shc-expressing cells after anti-oxidant treatment suggests that p66Shc may also decrease the activity of PMCAs besides its effects at the transcriptional level. In this context, we cannot exclude that the reduction in PMCA1/4 expression may be overestimated, as PMCA oxidation has been shown to result in the formation of insoluble aggregates that are eventually degraded.[36]

Although Ca^{2+} overload is known to activate the intrinsic apoptosis pathway,[19] the effects of p66Shc on Ca^{2+} homeo-stasis and mitochondrial function appear independent. p66Shc-expressing cells exposed to Trolox or subjected to long-term CsA treatment show indeed complete dissipation of mitochondrial transmembrane potential in response to A23187 notwithstanding normalization of the kinetics and extent of Ca^{2+} mobilization. Nevertheless, while the two pathways may be initially independent, they are likely to generate a feed-back amplification loop. Dissipation of the membrane potential minimizes the contribution of mitochondria to Ca^{2+} homeostasis and causes ATP depletion which may worsen Ca^{2+} overload by decreasing the fuel for the Ca^{2+} pumps. In turn, the alterations of Ca^{2+} homeostasis are likely to enhance the mitochondrial damage.

With the exception of the oxidizing activity on cytochrome c, all the known effects of p66Shc, including those described here, strictly require S36 phosphorylation.[4,6,7,9] Interestingly, we detected a significant fraction of S36-phosphorylated p66Shc under basal conditions. In a possible scenario, the

increased ROS production by p66Shc may cause functional PMCA impairment and increase resting $[Ca^{2+}]_c$. The resulting enhancement in calcineurin activity and NF-AT translocation would then be the initiating event leading to the decreased PMCA4a synthesis that predisposes p66Shc-expressing cells to Ca^{2+} overload. Furthermore, mitochondrial dysfunction might be initiated by cytochrome *c* release due to increased Bax expression and cardiolipin peroxidation. Together, these events would synergize in sensitizing p66Shc-expressing cells to apoptosis.

Materials and Methods

Cells, antibodies and chemicals. The cell lines used are derivatives of the Jurkat T cell lymphoma line stably transfected with either empty vector or expression constructs encoding p66Shc or a p66Shc mutant carrying a serine to alanine substitution at position 36 (p66SA).[4] Cell viability was measured by Trypan blue exclusion.

p66Shc/p66SA were immunoprecipitated using a rabbit polyclonal antiserum raised against a CH2-GST fusion protein.[6] Shc was probed by immunoblot using either monoclonal (Becton-Dickinson Biosciences Italia SpA, Milan, Italy) or polyclonal (Upstate Biotechnology Inc., Boston, MA, USA) antibodies raised against the Shc SH2 domain. A mAb recognizing phosphorylated S36 was purchased from Alexis Biochemicals (San Diego, CA, USA). Anti-Erk2, anti-cytochrome *c* and anti-PMCA1/4 antibodies were from Santa Cruz Biotechnology (Santa Cruz, CA, USA); anti-Fyn antibodies from Becton-Dickinson Biosciences and anti-actin mAb from Chemicon Europe Ltd (Chandlers Ford, UK). IgG from OKT3 (anti-human CD3, ATCC) hybridoma supernatants were affinity-purified on Mabtrap (Amersham Biosciences) and titrated by flow cytometry. Fluorochrome-labeled annexin V was purchased from Becton-Dickinson Biosciences Italia SpA (Milan, Italy). Secondary unlabeled antibodies were purchased from Cappel (Durham, NC, USA), secondary peroxidase-labeled antibodies from Amersham Biosciences.

A23187, thapsigargin, CsA, aristolochic acid, MK886, indomethacin, sodium vanadate, luciferase, D-luciferin and coenzyme A were purchased from Sigma-Aldrich srl (Milan, Italy); Trolox from Merck Biosciences GmbH (Schwalbach, Germany). Sanglifherin A was generously provided by Novartis Pharmaceuticals.

Flow cytometry. Flow cytometry was carried out using a FACScan flow cytometer (Becton-Dickinson, San Jose, CA, USA) equipped with a 15-mW 488 nm argon ion laser. The green (FL1) and orange (FL2) fluorescences were collected through a 530/30 and a 585/42 band pass filter, respectively. Data acquisition was performed using CellQuest software. Data were analysed and plotted using Flowjo (Tree Star, Inc.).

Phosphatidylserine exposure to the cell surface was quantitated using FITC-labeled annexin V (FL1).

$[Ca^{2+}]_c$ was measured using Fluo-4FF,AM (Molecular Probes Europe BV, Leiden, the Netherlands) (FL1). Cells (10^6/sample) were suspended in 200 μl RPMI 1640 w/o phenol Red (Invitrogen srl) added with 25 mM Hepes pH 7.4, 5 μM Fluo-4 and 500 μM sulfinpyrazone (Sigma-Aldrich srl). Cells were incubated 40 min at 37°C, pelleted by centrifugation and resuspended in 1 ml of the same medium without Fluo-4. Baseline fluorescence was recorded for 40 s at 37°C. Cells were subsequently added with either A23187 (500 ng/ml), thapsigargin (2 μM) or saturating amounts of anti-CD3 mAb and 50 μg/ml secondary antibody. Fluorescence was continously recorded for 512 s at 37°C. When pharmacological inhibitors were used, carrier or inhibitor was added to the culture medium and cells were incubated at 37°C for the appropriate time before loading with fluo-4.

Mitochondrial membrane potential was measured using the fluorescent probe, TMRM (Molecular Probes Europe BV) (FL2). Cells (10^6/sample) were suspended in 200 μl RPMI 1640 w/o phenol Red (Invitrogen srl) added with 25 mM Hepes pH 7.4 and 200 nM TMRM and incubated for 20 min at 37°C. Cells were diluted to 1 ml with RPMI 1640 w/o phenol Red added with 25 mM Hepes pH 7.4 and subjected to flow cytometric analysis. Pharmacological inhibitors were used as above. To induce AICD, cells were treated for 24–48 h with saturating amounts of plate-bound anti-CD3 mAb as described[4] and analyzed either as such or after restimulation for 6 h. CD3 was found to be expressed at similar levels on the surface of control and p66Shc-expressing cells after the long-term treatment with anti-CD3 mAb.

Transfections and confocal microscopy. Cells were transiently transfected with the plasmid pEGFP/NFAT-1D using a modification of the DEAE/dextran procedure, as described.[37] Confocal microscopy was carried out on a Leica TCS 4D laser scanning confocal microscope equipped with an argon-krypton laser and coupled to a Leica DMRBE microscope equipped with 63 × PL Apo 1.4 objectives (Leica Microsystems Heidelberg, Germany). Images collected at several focal planes were superimposed and merged into a single file using Confocal Assistant Software 4.02 (Biorad Laboratories srl, Milan, Italy) and subsequently imported into Adobe Photoshop (Adobe Systems Europe Ltd, Edinburgh, UK).

Ultrathin sections and electron microscopy. Cell pellets were fixed for 1 h at 4°C in 2.5% glutaraldehyde diluted in PBS, washed in buffer overnight, and postfixed in 1% osmium tetroxide for 1 h at 4°C. After one further rinse in buffer, samples were dehydrated with a graded series of ethanols and embedded in Epon-Araldite. Thin sections were obtained with a Reichert Ultracut II E ultramicrotome and recovered on 100 mesh copper grids. Sections were routinely stained with uranyl acetate and lead citrate and observed with a Philips CM10 transmission electron microscope with an electron accelerating voltage of 80 kV.

Immunoprecipitations, immunoblots, cell fractionations and cellular ATP measurements. Cells (1–5 × 10^6/sample for direct immunoblot analysis, 1–5 × 10^7/sample for immunoprecipitations) were lysed in 1% (v/v) Triton X-100 in 20 mM Tris-HCl pH 8, 150 mM NaCl (in the presence of 0.2 mg/ml Na orthovanadate, 1 μg/ml pepstatin, leupeptin and aprotinin and 10 mM PMSF) and postnuclear supernatants were probed as such or immunoprecipitated using the appropriate polyclonal antibodies and protein-A-Sepharose (Amersham Biosciences) as described.[4] Immunoblots were carried out using a chemiluminescence detection system (Pierce, Rockford, IL, USA). Immuno-reactive bands were quantitated by laser densitometry (Kodak Digital Science™ Electrophoresis Documentation and Analysis System 120).

Lipid rafts were purified by density gradient centrifugation from 50 × 10^6 cells/sample lysed out at 37°C using 1% Brij-98, and proteins from the pooled low-density raft-enriched fractions were extracted and concentrated as described.[38]

Post-mitochondrial supernatants were obtained by cell fractionation using a modification of the protocol described by Liang *et al*.[39] Briefly, 30 × 10^6 cells/sample were washed twice with PBS, resuspended in 450 μl buffer A (20 mM Hepes pH 7.0, 10 mM KCl, 1.5 mM MgCl$_2$, 1 mM EDTA, 1 mM EGTA, 1 mM DTT, 0.1 mM PMSF, 250 mM sucrose), incubated 10 min on ice and broken in a Dounce homogenizer (25 strokes). The homogenate was centrifuged at 4°C for 10 min at 600 × *g*, and the supernatant was subjected to a second centrifugation at 4°C for 10 min at 700 × *g*. The latter supernatant was then centrifuged at 4°C for 10 min at 7000 × *g*. The pellet, enriched in mitochondria, was discarded, whereas the post-mitochondrial supernatant was used for immunoblot analysis of cytochrome *c* release.

Cellular ATP was measured using a luciferase-based assay. Cells/sample (2 × 10^6) were resuspended in 40 μl 100 mM Tris, 4 mM EDTA, pH 7.75 and lysed by boiling for 4 min. Samples were centrifuged for 1 min at 10 000 × *g*; 10 μl of the supernatants was added with 200 μl luciferase assay buffer (20 mM Tricine, 1.07 mM (MgCO$_3$)$_4$Mg(OH)$_2$ · 5H$_2$O, 2.67 mM MgSO$_4$, 0.1 mM EDTA, 33.3. mM DTT, 270 μM coenzyme A, 470 μM D-luciferin, pH 7.8) and 10 ng luciferase. Light emission was immediately recorded as relative light units using a Bioorbit 1253 luminometer.

RT-PCR. Semiquantitative RT-PCR was carried out using total RNA extracted using the RNA WIZ™ isolation reagent (Ambion Inc., Austin, TX, USA). RT-PCR was carried out using AMV reverse transcriptase and the Expand High Fidelity PCR system from Roche Diagnostics SpA (Milan, Italy). The primer for the first strand was oligo-dT (Promega Italia srl, Milan, Italy), while pairs of primers specific for human *PMCA1b*, *4a* and *4b* were used for cDNA amplification. Actin was used as housekeeping control. cDNA was amplified in an Eppendorf Mastercycler Thermal Cycler (Eppendorf srl, Milan, Italy). The RT-PCR products were separated by agarose gel electrophoresis, and the intensities of the PMCA and actin-specific bands was quantitated by laser densitometry. The relative levels of PMCA mRNA were normalized to the levels of actin mRNA.

1. Ravichandran KS. Signaling via Shc family adapter proteins. *Oncogene* 2001; **20**: 6322–6330.
2. Migliaccio E, Mele S, Salcini AE, Pelicci G, Lai KM, Superti-Furga G *et al*. Opposite effects of the p52shc/p46shc and p66shc splicing isoforms on the EGF receptor-MAP kinase-fos signalling pathway. *EMBO J* 1997; **16**: 706–716.
3. Okada S, Kao AW, Ceresa BP, Blaikie P, Margolis B, Pessin JE. The 66-kDa Shc isoform is a negative regulator of the epidermal growth factor-stimulated mitogen-activated protein kinase pathway. *J Biol Chem* 1997; **272**: 28042–28049.
4. Pacini S, Pellegrini M, Migliaccio E, Patrussi L, Ulivieri C, Ventura A *et al*. p66SHC promotes apoptosis and antagonizes mitogenic signaling in T cells. *Mol Cell Biol* 2004; **24**: 1747–1757.
5. Pellegrini M, Pacini S, Baldari CT. p66SHC: the apoptotic side of Shc proteins. *Apoptosis* 2005; **10**: 13–18.
6. Migliaccio E, Giorgio M, Mele S, Pelicci G, Reboldi P, Pandolfi PP *et al*. The p66shc adaptor protein controls oxidative stress response and life span in mammals. *Nature* 1999; **402**: 309–313.
7. Smith WW, Norton DD, Gorospe M, Jiang H, Nemoto S, Holbrook NJ *et al*. Phosphorylation of p66Shc and forkhead proteins mediates Aβ toxicity. *J Cell Biol* 2005; **169**: 331–339.
8. Yang CP, Horwitz SB. Taxol mediates serine phosphorylation of the 66-kDa Shc isoform. *Cancer Res* 2000; **60**: 5171–5178.
9. Nemoto S, Finkel T. Redox regulation of forkhead proteins through a p66shc-dependent signaling pathway. *Science* 2002; **295**: 2450–2452.
10. Trinei M, Giorgio M, Cicalese A, Barozzi S, Ventura A, Migliaccio E *et al*. A p53-p66Shc signalling pathway controls intracellular redox status, levels of oxidation-damaged DNA and oxidative stress-induced apoptosis. *Oncogene* 2002; **21**: 3872–3878.
11. Napoli C, Martin-Padura I, de Nigris F, Giorgio M, Mansueto G, Somma P *et al*. Deletion of the p66Shc longevity gene reduces systemic and tissue oxidative stress, vascular cell apoptosis, and early atherogenesis in mice fed a high-fat diet. *Proc Natl Acad Sci USA* 2003; **100**: 2112–2116.
12. Zaccagnini G, Martelli F, Fasanaro P, Magenta A, Gaetano C, Di Carlo A *et al*. p66ShcA modulates tissue response to hindlimb ischemia. *Circulation* 2004; **109**: 2917–2923.
13. Orsini F, Migliaccio E, Moroni M, Contursi C, Raker VA, Piccini D *et al*. The life span determinant p66Shc localizes to mitochondria where it associates with mitochondrial heat shock protein 70 and regulates trans-membrane potential. *J Biol Chem* 2004; **279**: 25689–25695.
14. Bernardi P, Krauskopf A, Basso E, Petronilli V, Blalchy-Dyson E, Di Lisa F *et al*. The mitochondrial permeability transition from *in vitro* artifact to disease target. *FEBS J* 2006; **273**: 2077–2099.
15. Giorgio M, Migliaccio E, Orsini F, Paolucci D, Moroni M, Contursi C *et al*. Electron transfer between cytochrome *c* and p66(Shc) generates reactive oxygen species that trigger mitochondrial apoptosis. *Cell* 2005; **122**: 221–223.
16. Ventura A, Luzi L, Pacini S, Baldari CT, Pelicci PG. The p66Shc longevity gene is silenced through epigenetic modifications of an alternative promoter. *J Biol Chem* 2002; **277**: 22370–22376.
17. Penzo D, Petronilli V, Angelin A, Cusa C, Colonna R, Scorrano L *et al*. Arachidonic acid released by phospholipase A(2) activation triggers Ca(2+)-dependent apoptosis through the mitochondrial pathway. *J Biol Chem* 2004; **279**: 25219–25225.
18. Bernardi P. Mitochondrial transport of cations: channels, exchangers and permeability transition. *Physiol Rev* 1999; **79**: 1127–1155.
19. Orrenius S, Zhivotovsky B, Nicotera P. Regulation of cell death: the calcium-apoptosis link. *Nat Rev Mol Cell Biol* 2003; **4**: 552–565.
20. Scorrano L, Oakes SA, Opferman JT, Cheng EH, Sorcinelli MD, Pozzan T *et al*. BAX and BAK regulation of endoplasmic reticulum Ca2+: a control point for apoptosis. *Science* 2003; **300**: 135–139.
21. Bautista DM, Hoth M, Lewis RS. Enhancement of calcium signalling dynamics and stability by delayed modulation of the plasma-membrane calcium-ATPase in human T cells. *J Physiol* 2002; **541**: 877–894.
22. Chen J, McLean PA, Neel BG, Okunade G, Shull GE, Wortis HH. CD22 attenuates calcium signaling by potentiating plasma membrane calcium-ATPase activity. *Nat Immunol* 2004; **5**: 651–657.
23. Fujimoto T. Calcium pump of the plasma membrane is localized in caveolae. *J Cell Biol* 1993; **120**: 1147–1157.
24. Guerini D, Wang X, Li L, Genazzani A, Carafoli E. Calcineurin controls the expression of isoform 4CII of the plasma membrane Ca(2+) pump in neurons. *J Biol Chem* 2000; **275**: 3706–3712.
25. Rao A, Luo C, Hogan PG. Transcription factors of the NFAT family: regulation and function. *Annu Rev Immunol* 1997; **15**: 707–747.
26. Eskes R, Desagher S, Antonsson B, Martinou JC. Bid induces the oligomerization and insertion of Bax into the outer mitochondrial membrane. *Mol Cell Biol* 2000; **20**: 929–935.
27. Gross A, Jockel J, Wei MC, Korsmeyer SJ. Enforced dimerization of BAX results in its translocation, mitochondrial dysfunction and apoptosis. *EMBO J* 1998; **17**: 3878–3885.
28. Cai J, Jones DP. Superoxide in apoptosis. Mitochondrial generation triggered by cytochrome *c* loss. *J Biol Chem* 1998; **273**: 11401–11404.
29. Scorrano L, Ashiya M, Buttle K, Weiler S, Oakes SA, Mannella CA *et al*. A distinct pathway remodels mitochondrial cristae and mobilizes cytochrome *c* during apoptosis. *Dev Cell* 2002; **2**: 55–67.
30. Soriano ME, Nicolosi L, Bernardi P. Desensitization of the permeability transition pore by cyclosporin A prevents activation of the mitochondrial apoptotic pathway and liver damage by tumor necrosis factor-alpha. *J Biol Chem* 2004; **279**: 36803–36808.
31. Chiara MD, Bedoya F, Sobrino F. Cyclosporin A inhibits phorbol ester-induced activation of superoxide production in resident mouse peritoneal macrophages. *Biochem J* 1989; **264**: 21–26.
32. Guerini D, Pan B, Carafoli E. Expression, purification, and characterization of isoform 1 of the plasma membrane Ca^{2+} pump: focus on calpain sensitivity. *J Biol Chem* 2003; **278**: 38141–38148.
33. Schwab BL, Guerini D, Didszun C, Bano D, Ferrando-May E, Fava E *et al*. Cleavage of plasma membrane calcium pumps by caspases: a link between apoptosis and necrosis. *Cell Death Differ* 2002; **9**: 818–831.
34. Heissmeyer V, Macian F, Im SH, Varma R, Feske S, Venuprasad K *et al*. Calcineurin imposes T cell unresponsiveness through targeted proteolysis of signaling proteins. *Nat Immunol* 2004; **5**: 255–265.
35. Bigelow DJ, Squier TC. Redox modulation of cellular signaling and metabolism through reversible oxidation of methionine sensors in calcium regulatory proteins. *Biochim Biophys Acta* 2005; **1703**: 121–123.
36. Zaidi A, Michaelis ML. Effects of reactive oxygen species on brain synaptic plasma membrane Ca(2+)-ATPase. *Free Radic Biol Med* 1999; **27**: 810–821.
37. Plyte S, Boncristiano M, Fattori E, Galvagni F, Rossi Paccani S, Majolini MB *et al*. Identification and characterization of a novel nuclear factor of activated T-cells-1 isoform expressed in mouse brain. *J Biol Chem* 2001; **276**: 14350–14358.
38. Ghittoni R, Patrussi L, Pirozzi K, Pellegrini M, Lazzerini PE, Capecchi PL *et al*. Simvastatin inhibits T-cell activation by selectively impairing the function of Ras superfamily GTPases. *FASEB J* 2005; **19**: 605–607.
39. Liang Y, Yan C, Nylander KD, Schor NF. Early events in Bcl-2-enhanced apoptosis. *Apoptosis* 2003; **8**: 609–611.